

Massively Parallel Recording of Unit and Local Field Potentials With Silicon-Based Electrodes

Jozsef Csicsvari,^{1,*} Darrell A. Henze,^{1,*} Brian Jamieson,^{2,*} Kenneth D. Harris,¹ Anton Sirota,¹ Péter Barthó,¹ Kensall D. Wise,² and György Buzsáki¹

¹Center for Molecular and Behavioral Neuroscience, Rutgers, The State University of New Jersey, Newark, New Jersey 07102; and

²Department of Electrical Engineering and Computer Science, The University of Michigan, Ann Arbor, Michigan 48109-2122

Submitted 8 February 2003; accepted in final form 17 April 2003

Csicsvari, Jozsef, Darrell A. Henze, Brian Jamieson, Kenneth D. Harris, Anton Sirota, Péter Barthó, Kensall D. Wise, and György Buzsáki. Massively parallel recording of unit and local field potentials with silicon-based electrodes. *J Neurophysiol* 90: 1314–1323, 2003; 10.1152/jn.00116.2003. Parallel recording of neuronal activity in the behaving animal is a prerequisite for our understanding of neuronal representation and storage of information. Here we describe the development of micro-machined silicon microelectrode arrays for unit and local field recordings. The two-dimensional probes with 96 or 64 recording sites provided high-density recording of unit and field activity with minimal tissue displacement or damage. The on-chip active circuit eliminated movement and other artifacts and greatly reduced the weight of the headgear. The precise geometry of the recording tips allowed for the estimation of the spatial location of the recorded neurons and for high-resolution estimation of extracellular current source density. Action potentials could be simultaneously recorded from the soma and dendrites of the same neurons. Silicon technology is a promising approach for high-density, high-resolution sampling of neuronal activity in both basic research and prosthetic devices.

INTRODUCTION

In the brain, there are both large- and small-scale levels of organization. It has been suggested that the cortex is constructed from building blocks (e.g., columns, barrels, lamellae) of similar intrinsic anatomical connections and functional properties (Andersen et al. 1969; Mountcastle 1997; Rice and Van der Loos 1977; Szentágothai 1975). This sub-millimeter level of organization is where computational rules of neuronal interactions are expected to reside (Churchland and Sejnowski 1992; Petsche et al. 1984). Several approaches have been introduced for achieving fast, parallel recording of neuronal elements. Optical imaging of multiple single neurons is a recent promising development in this field (Mao et al. 2001). However, this approach is not practical for monitoring deep cortical or subcortical activity in behaving animals. An alternative approach is to use multiple wire electrodes to record from large number of neurons simultaneously. Dozens of putative single cells have been recorded in rodents and hundreds in a primate using multiple wire electrodes (Csicsvari et al. 1999; Hoffman and McNaughton 2002; Wilson and McNaughton

1993, 1994). Several recent reviews have documented progress in this field (Chicurel 2001; Deadwyler and Hampson 1995; Eichenbaum and Davis 1988; Hampson et al. 2001; Nádasdy et al. 1998; Nicolelis et al. 1997).

Sharp wire or glass electrodes have the advantage of isolating single cells reliably (Evarts 1968; Lang et al. 1999). However, because of their high impedance, artifacts generated by the movement of the behaving animal are frequent. Furthermore, the proximity of the electrode tip to the neuron can mechanically stimulate it and change its firing properties. Importantly, multiple-unit recordings require multiple movable drives and wires, considerably increasing tissue damage. Monitoring the same neuronal pool with closely spaced multiple-site electrodes (“stereotrodes,” “tetrodes”) has greatly facilitated the unit yield/tissue damage ratio by introducing novel spike sorting (“unit clustering”) methods on the basis of the temporal coherence and waveform variance of spikes across multisite electrodes (Drake et al. 1988; Gray et al. 1995; McNaughton et al. 1983; Recce and O’Keefe 1989; Wilson and McNaughton 1993). Wire tetrodes have numerous advantages, including easy and cheap fabrication, low-impedance recording tips, and mechanical stability. However, the exact configuration of the recording tips relative to the neurons is not known (Jog et al. 2002). The spacing of multiple tetrodes is limited by the mechanical drives and the tissue damage they inflict. Importantly, each tetrode requires a separate drive for proper tip positioning and in situ buffering with external pre-amplifiers that require extensive connector wiring. These latter factors add substantially to the mass to be carried by the animal and severely limit the number of recording sites in freely moving small animals.

Micromachined silicon-based electrodes can eliminate or reduce some of the technical limitations inherent in multiple wire electrodes (Buzsáki et al. 1981; Drake et al. 1988; Kuperstein and Eichenbaum 1985; Petsche et al. 1984). In silicon devices, the thin-film recording sites are defined lithographically. Any two-dimensional configuration can be achieved with proper design and can be adapted to particular brain structures and neuron types. Silicon probes can be combined with on-chip integrated circuitry (Bai and Wise 2001; Olsson et al. 2002) to reduce cross-talk and spurious noise and perform anti-aliasing

*These authors contributed equally to this work.

G. Buzsáki, Center for Molecular and Behavioral, Neuroscience, Rutgers University, 197 University Ave., Newark, NJ 07102 (E-mail: Buzsaki@axon.rutgers.edu).

The costs of publication of this article were defrayed in part by the payment of page charges. The article must therefore be hereby marked “advertisement” in accordance with 18 U.S.C. Section 1734 solely to indicate this fact.

and impedance transformations. We have designed and tested two-dimensional probes with 64 and 96 recording sites and examined their field- and unit-recording abilities in the neocortex and hippocampus of the rat.

METHODS

Electrode configurations

Micro-electro-mechanical-system (MEMS)-based devices are particularly useful for simultaneous recording local field and unit activity from large numbers of sites with minimal damage to the nervous tissue. MEMS devices can combine silicon integrated-circuit processing with thin-film microelectrode sensing (see APPENDIX) (Gingerich et al. 2001; Najafi and Wise 1986; Wise and Najafi 1991).

In the present experiments, three different types of two-dimensional micromachined probes were examined. The first probe was designed primarily to record extracellular currents in the hippocampus and neocortex of the rat. It contained six shanks (300- μm shank separation) and each shank had 16 iridium recording sites (108 μm^2) with 100- μm vertical spacing (Fig. 1A). The interconnects (2 μm wide and 2 μm spacing) were passivated by a dielectric layer formed by stress-balanced stack of silicon dioxide and silicon nitride chemical vapor deposited films. The 12- μm -thick shanks tapered from a maximum width of 85 μm at the base to a sharp tip. The two-dimensional extent of the probe sampled the CA1, CA3 regions and the dorsal part of the dentate gyrus (Fig. 2). The second array consisted of eight shanks (200- μm shank separation) and each shank had eight recording sites (160 μm^2) with 50- μm vertical spacing (Fig. 1B1). This probe was designed primarily for high-density recording of unit activity and extracellular current activity in the neocortex and hippocampus. The configuration of the third probe was similar to the second but the recordings sites were staggered to provide a two-dimensional arrangement of the tips (20 μm vertical separation; Fig. 1B2). Both "passive" and "active" configurations were tested. Active probes had on-chip preamplifiers (Fig. 1, C and D) to reduce movement-associated artifacts. The probes were attached to a stereotaxic drive (acute experiments) or a microdrive (chronic experiments), which allowed us to position the probes to the desired target depth during the experiment.

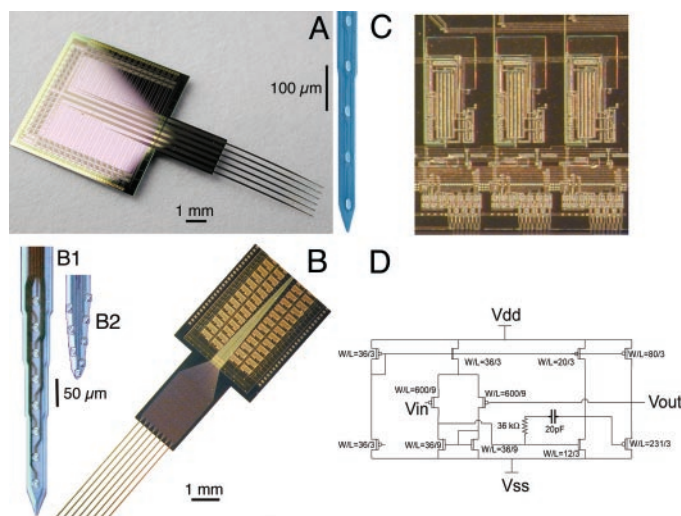


FIG. 1. Multiple-site recording probes. *A*: 6-shank, 96-site passive probe for 2-dimensional imaging of field activity. Recording sites (16 each; 100 μm vertical spacing) are shown at higher magnification. *B*: 8-shank, 64-site active probe. Two different recording site configurations (linear, *B1* and staggered sites, *B2*) are shown as insets. *C*: close-up of on-chip buffering circuitry. Three of the 64 amplifiers and associated circuits are shown. *D*: circuit schematic of operational amplifier for buffering neural signals.

Surgery and recording

For acute recordings, Sprague-Dawley rats (Hilltop laboratories or Zivic Miller laboratories) 300–500 g were anesthetized with urethan (1.5 g/kg) and placed in a stereotaxic frame. After preparing a 1 \times 3-mm window in the skull, the dura was removed using a dissection microscope and the probe was positioned so that the tips avoided blood vessels. The skull cavity was filled with a mixture of wax and paraffin which decreased brain pulsation as well as provided lateral support for the probe shanks. The probe was attached to a micromanipulator and moved gradually to its desired depth position. The middle shanks were centered at anterior-posterior, AP = -3.5 mm and mediolateral, ML = 2.5 mm position. Extracellular units and local field were recorded by the silicon probes from either the somatosensory cortex or the hippocampus. After each acute experiment, the probe was rinsed with deionized water. Probes were used repeatedly for several months without noticeable deterioration in performance. A pair of stainless steel wires (60 μm in diameter) was placed into the fimbria-fornix/hippocampal commissure (AP = -0.8 , L = 0.5, V = -4.2 mm) to stimulate the commissural afferents to the hippocampus. Extracellular signals were high-pass filtered (1Hz) and amplified (1,000 times) using a 64-channel amplifier (Sensorium, Charlotte, VT). All data were digitized at 20 kHz (DataMax System, RC Electronics, Santa Barbara, CA) and stored on computer disk for later analysis.

The general surgical procedures for chronic recordings have been described (Csicsvari et al. 2003). In short, rats of the Sprague-Dawley strain (400–900 g) were anesthetized with a mixture (4 ml/kg) of ketamine (25 mg/ml), xylazine (1.3 mg/ml), and acepromazine (0.25 mg/ml) and placed in the stereotaxic apparatus. The probes were attached to a custom-prepared microdrive. The probes were implanted the same way as in the acute experiments. During implantation, the tips of the probe shanks were lowered ~ 400 μm below the brain surface. After recovery from surgery, the probes were moved gradually and recordings were made at several depth locations. A pair of stainless steel wires (60 μm in diameter) were placed into the fimbria-fornix/hippocampal commissure (AP = -0.8 , L = 0.5, V = -4.2 mm) to stimulate the commissural afferents to the hippocampus and another pair in the angular bundle (AP = -7.0 , L = 4.5, V = -3.5 mm) to stimulate the entorhinal input. The evoked responses by these pathways helped the on-line identification of the recording electrodes (Bragin et al. 1995). All procedures conformed to the National Institutes of Health Guide for the Care and Use of Laboratory Animals.

The physiological data were collected during spontaneous exploration on open field and during sleep episodes in the home cage. With passive probes, instrumentation amplifiers, built into the female connector (Szabó et al. 2001), were used to reduce cable movement artifacts. Two synchronized 64-channel DataMax systems (16-bit resolution; RC Electronics, Santa Barbara, CA) continuously recorded electrical activity at 20 kHz to computer hard disk.

SPIKE SORTING. The continuously recorded wide-band signals were high-pass filtered (0.8–5 kHz) digitally. Units were initially isolated by an automatic algorithm ("KlustaKwik," available at: <http://osiris.rutgers.edu/Buzsaki/software>) followed by manual clustering (Csicsvari et al. 1998). Auto- and cross-correlations were calculated to verify the clustering procedure.

CURRENT SOURCE DENSITY (CSD) ANALYSIS. One-dimensional CSD maps were calculated in one direction (depth) as the second spatial derivative of the local field potentials (Nicholson and Freeman 1975). This approach assumes that the resistivity of the extracellular medium is homogeneous and isotropic. Although some resistivity differences are present in the different hippocampal layers, in practice these are not large enough to significantly modify the spatial distribution of sinks and sources (Holsheimer 1987).

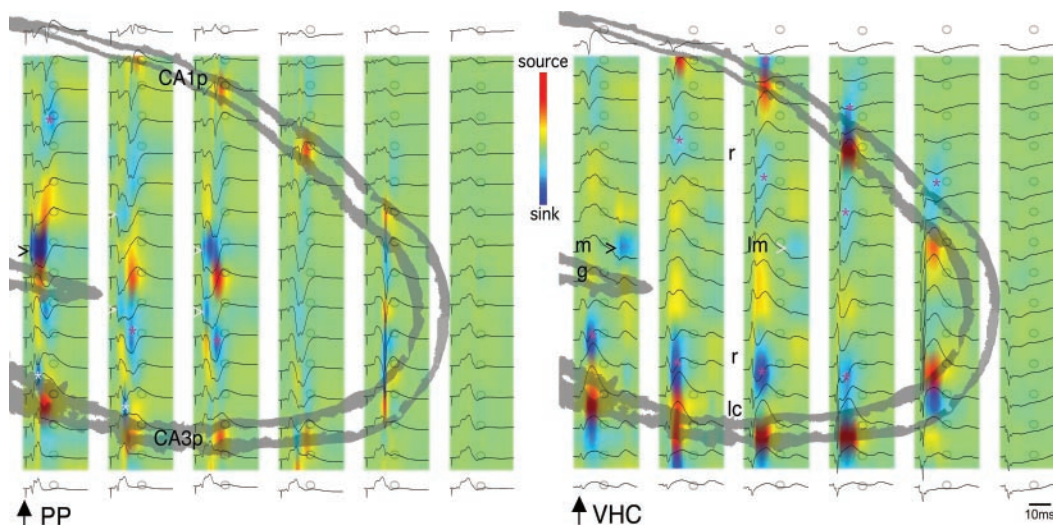


FIG. 2. On-line calibration of recording site positions. Single evoked responses in response to perforant path or ventral hippocampal commissure (VHC) stimulation (vertical arrows) recorded at 96-sites simultaneously in the freely moving rat. Gray circles, recording sites superimposed on a histological section containing the probe shanks (cell body layers outlined in gray). Each shank had 16 recording sites at 100 μm vertical spacing with 300- μm intervals between shanks. Color panels: CSD maps derived from the evoked field responses. Note that large sources (hot colors) outline the cell body layers. Black and white arrowheads, perforant path-evoked sink currents in the middle molecular layer of the dentate gyrus and CA3 stratum lacunosum-moleculare, respectively. White asterisk, mossy fiber evoked sinks in CA3 str. lucidum. Magenta asterisk, di- and trisynaptically evoked sinks in CA3 and CA1 regions, respectively. CA1p, CA3p, CA1 and CA3 pyramidal layer, respectively; g, granule cell layer; m, molecular layer; r, str. radiatum; l-m, str. lacunosum-moleculare; lc, str. lucidum.

Histological procedures

After completion of the experiments, the rats were deeply anesthetized and perfused through the heart first with 0.9% saline solution followed by a 10% buffered formalin phosphate solution. The brains were sectioned by a Vibroslice at 100 μm in the coronal plane. The sections were mounted on slides, Nissl-stained, and coverslipped. The tracks of the silicon probe shanks were reconstructed from multiple sections. DiI labeling around the shanks were viewed with a fluorescence microscope. The exact recording sites in the vertical direction for each session were determined by the evoked responses. The derived electrical patterns then were superimposed on the anatomical substrate that emanated them.

RESULTS

On-line estimation of the recording site positions

The 96-site probe provided a two-dimensional image of electrical activity (1.6 mm deep, 1.8 mm wide area) across several subregions of the hippocampus in the behaving rat. Electric stimulation of the entorhinal (perforant path) and commissural/associational afferents, with known spatial distribution and targets, provided a tool for a reliable calibration of the recording sites (Fig. 2) (Ylinen et al. 1995). The evoked sink and source currents (estimated from the field potentials; see METHODS) precisely identified the activated layers. In response to perforant path stimulation, monosynaptic excitatory responses were evoked in the granule cell dendrites and the distal apical dendrites of CA3 pyramidal cells (sinks indicated by arrowheads in Fig. 2, *left*) (Andersen et al. 1971; Do et al. 2002). Stronger stimulation evoked population responses of the granule cells, followed by di- and trisynaptic activation of CA3 and CA1 pyramidal cells, respectively. The sink-associated sources in the cell body layers reliably identified the CA3–CA1 pyramidal cell layers and the dentate granule cell layer. Stim-

ulation of commissural fibers evoked antidromic discharge of CA3 pyramidal cells. Sinks at monosynaptic latency were present in CA3 and CA1 dendritic layers. Stronger stimulation induced orthodromic population spikes and, occasionally, a reverberating, entorhinal cortex-mediated late response (Fig. 2, *right*; arrowhead). In addition to the evoked responses, the presence of multiple-unit discharges at several sites helped identify the pyramidal and granule cell layers. Large-amplitude field ripples (140–200 Hz) during immobility provided additional information for the identification of CA1 pyramidal layer (Buzsáki et al. 1992). At the termination of the experiments, the brain was perfused with the probe left in situ. Histological localization of the electrode tracks was used to verify the prediction of the recording sites. In all six rats, there was a perfect match between the physiology-predicted and histologically identified sites of the probe. Once the two-dimensional positions of the recording sites were determined, spontaneously occurring patterns (e. g., theta, gamma, sharp wave-ripples) were recorded and their sink-source distributions were related to the known anatomical afferents (Csicsvari et al. 2003). The approach illustrated in the preceding text can be used for on-line “calibration” in the neocortex as well, using thalamic and callosal inputs (Castro-Alamancos and Connors 1996; Kandel and Buzsáki 1997).

Although the spacing of the recording sites (100 μm) on the 96-site probes is not ideal for hippocampal unit separation, typically two neighboring sites on an individual shank recorded from the same units in the CA1–CA3 pyramidal cell layers. Unit clustering with such “stereotrode” configuration (McNaughton et al. 1983) yielded ≥ 60 clear unit clusters in the hippocampus of the behaving rat. For clustering neocortical pyramidal cells with long apical shafts, the 100- μm recording-site separation appeared adequate. In fact, many single neurons could be recorded from four to six sites (Buzsáki and Kandel

1998). In some shanks, every single site recorded some unit activity and as many as 20 unit clusters could be separated by a single shank in the neocortex. Because the two-dimensional spatial position of the recorded units can be precisely determined with the 96-site probes, these measurements will allow for quantitative studies of the intra- and inter-columnar interactions of cortical neurons.

Field and unit recordings by 64-site probes

Figure 3 illustrates recordings with the 64-site probe (staggered recording sites; Fig. 1B2) from deep layers of the somatosensory cortex of the urethane-anesthetized rat. The alternation of active and silent periods at ~ 0.5 Hz reflects slow oscillations characteristic of the anesthetized brain (Fig. 3A) (Steriade 2001). All 64 recording sites yielded unit activity, and the same units were recorded by several recording sites of the same shank (Fig. 3B). The spike amplitude and waveform of the neuron varied across recording sites. The voltage gradient of spikes across the recording sites provided an approximate location of the cell body of the recorded neuron. The spike amplitude from presumed perisomatic locations often exceeded 0.3 mV.

Using probes with linearly arranged recording sites (Fig. 1B1), the speed of soma-dendritic back-propagation of the action potentials could be measured for numerous neurons (Fig. 4A) (Buzsáki and Kandel 1998). In future experiments, this will allow for the examination of behavior modulation of back-propagating action potentials (Buzsáki et al. 1996; Harris et al. 2001; Quirk et al. 2001). Nine to 18 neurons per shank

could be routinely discriminated. Due to the high spatial density of the recording sites, the relative vertical position of the recorded units could be reliably determined (Fig. 4B). This feature will be useful in determining spatiotemporal activation on neuronal populations under physiological conditions. The sufficiently large number of recording sites per shank also yielded a high-resolution CSD of various local field potentials (not shown). This important feature of the 64-site probe should be emphasized because local inhomogeneities in field potential generation and the contribution of unit discharge patterns to the generation of local field can now be rigorously studied (Pesaran et al. 2002).

Probes with on-chip active circuitry had two major advantages in chronically implanted animals. First, the preamplifier head-stage was eliminated, and therefore the rat had to carry substantially less bulk. Second, the interconnect between the high-impedance recording sites ($1\text{--}3\text{ M}\Omega$ at 1,000 Hz) and the preamplifier input was reduced to <6 mm. A large part of this interconnect was shielded by the brain. The length of the interconnect is critical because it serves as an “antenna” and introduces large slow-frequency artifacts, originating from movement of the electrically charged whiskers, cable movements, fast head movement-associated “microphonia,” and other environmental noise sources. Although these artifactual sources pose less of a problem for unit recordings, they can effectively prevent proper detection and interpretation of field potentials at low frequencies. Using the active probes, we obtained artifact-free recordings even during vigorous movements or jumps (Fig. 5). Because the physical location of the

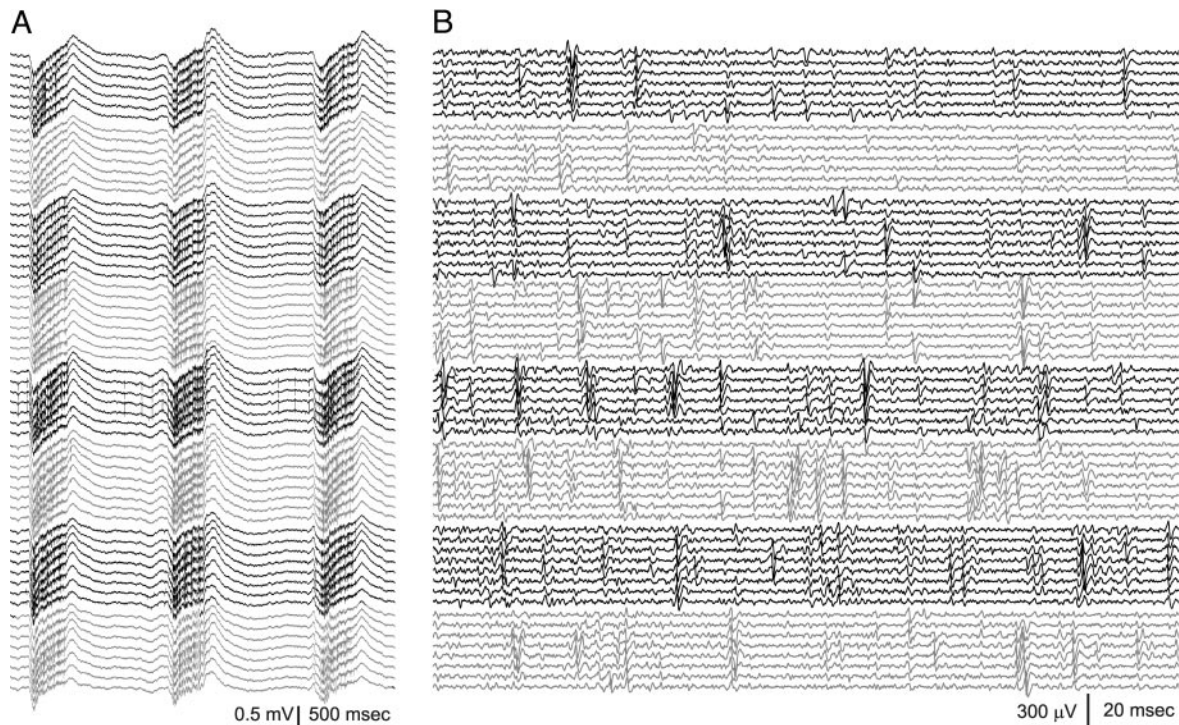


FIG. 3. Parallel recording of unit activity in layer V of the somatosensory cortex. *A*: wide-band recording of field and unit activity by a 64-channel (staggered sites) probe under urethane anesthesia. Recordings from the 8 parallel shanks, positioned in layer V, are plotted below each other. *Top*: leftmost shank; *bottom*, rightmost shank. Note coherent, rhythmic alteration of population activity and neuronal silence at all recording sites (corresponding to “up-down” cortical states) (Steriade 2001). *B*: filtered traces (500 Hz to 5 kHz) corresponding to traces shown in *A* at faster speed, highlighting unit discharges during “up” state. Note that action potentials are simultaneously present on several recording sites of a given shank.

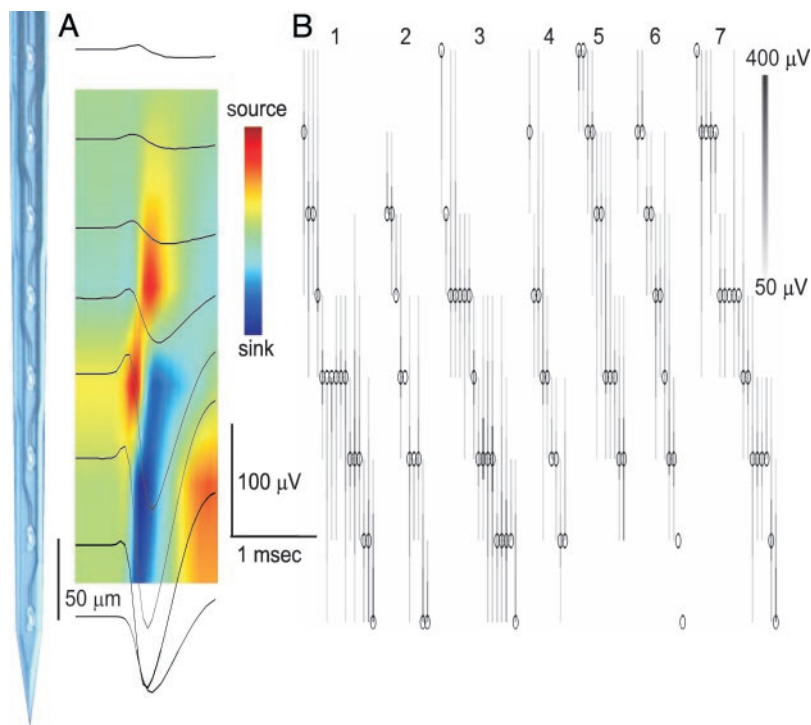


FIG. 4. Unit distribution in 2-dimensional space. *A*: wide-band (1 Hz to 5 kHz) averaged traces of a single, layer V unit (black traces) and the derived current source density (CSD) map of the action potential. Note somadendritic propagation of the spike. Recordings were made with a 64-channel (linear sites) probe (1 shank is shown). *B*: for the determination of the vertical position of neuron, the site with the largest amplitude signal was regarded as the approximate location of the cell body (ellipses) (Henze et al. 2000). Unit amplitude distribution on neighboring recording sites is illustrated with different shades of gray. Shank numbers are indicated on top (1–7; data from shank 8 are missing).

recorded neurons can be reliably predicted, this device will be useful to address issues like spatial extent of inhibition and organization of hippocampal representations (Hampson et al. 1999; Hirase et al. 2001; Redish et al. 2001).

Unit isolation

Silicon probes offer a unique opportunity for massively parallel unit recordings. Given the relatively large vertical span of the eight-site shanks (350 or 140 μm), routinely five to seven shanks could be positioned in the CA1 pyramidal layer. Shanks spanning the pyramidal layer typically recorded 8–15 high-quality units, i.e., the same number or more than from an average wire tetrode. The quality of the isolated units was quantitatively determined using the “isolation distance” measure of unit quality (Fig. 6, *inset*) (Harris et al. 2001). This measure indicated that unit-isolation quality was similar to those obtained by wire tetrodes (Fig. 6).

Full utilization of the power of silicon probes, however, requires advanced methods of spike detection and cluster isolation. First, when using such a large-dimensional feature space, automatic cluster separation is a necessity. Software for this approach is available (Harris et al. 2000). However, silicon probes pose new challenges for which spike-sorting methods, developed for wire tetrodes, may not be optimal. In particular, tetrode spike detection typically cannot identify spikes of different cells that occur within ~ 1 ms of each other due to the problem of resolving overlapping spikes. With the silicon probes this problem is more serious because larger numbers of recorded cells are associated with more overlapping spikes. However, this problem is potentially solvable because the different cells may be measured on different sites. Furthermore because each cell is detectable, only on some of the channels, including channels that do not record from a particular cell add unnecessary noise. Spike-sorting methods that take advantage

of the additional spatial and temporal information afforded by the silicon arrays are needed to exploit the full potentials of silicon probes.

Tissue displacement/damage by silicon probes

Histological examination of the electrodes revealed very little effect on brain tissue. In contrast to wire tetrodes with blunt cut ends, it was possible to record from the same cell layer numerous times after moving the probe up and subsequently back to the previous recording locations. Recordings from isolated single units showed that the same cell could be recorded from by several successive sites while the probe was moved by 50- μm steps. Focal bleeding from capillaries around the tracks was very rare. In fact, after acute recordings, the electrode track could not be recovered in most cases because in the absence of gliosis no other landmarks identified the tracks. In subsequent experiments, the shanks were dipped into concentrated DiI solution and dried prior to implantation. This procedure did not interfere with the recording qualities of the probes, and the tracks could be positively identified by the vertical bands of fluorescent processes. In chronic experiments, the tracks could be recognized by the tissue indent left by the shanks (Csicsvari et al. 2003). No obvious tissue reaction was visible around the tracks, in support of a recent detailed report on the biocompatibility of silicon-based devices (Kristensen et al. 2001).

Although moving the eight-site shanks (62 μm wide at the top recording site) up and down in the tissue several times yielded apparently the same units, in experiments with the 16-site probes, we noticed that when recordings sites 12–16 penetrated through the CA1 pyramidal cell layer, the quality of units deteriorated. Similar deterioration of unit quality was obvious also in cortical layers II and III. The width of the 16-site probe at the 16th recording site is 82 μm (12- μm thick). Thus we believe that the main cause of the reduction of unit quality is due to the tissue damage caused by the widening of the shank.

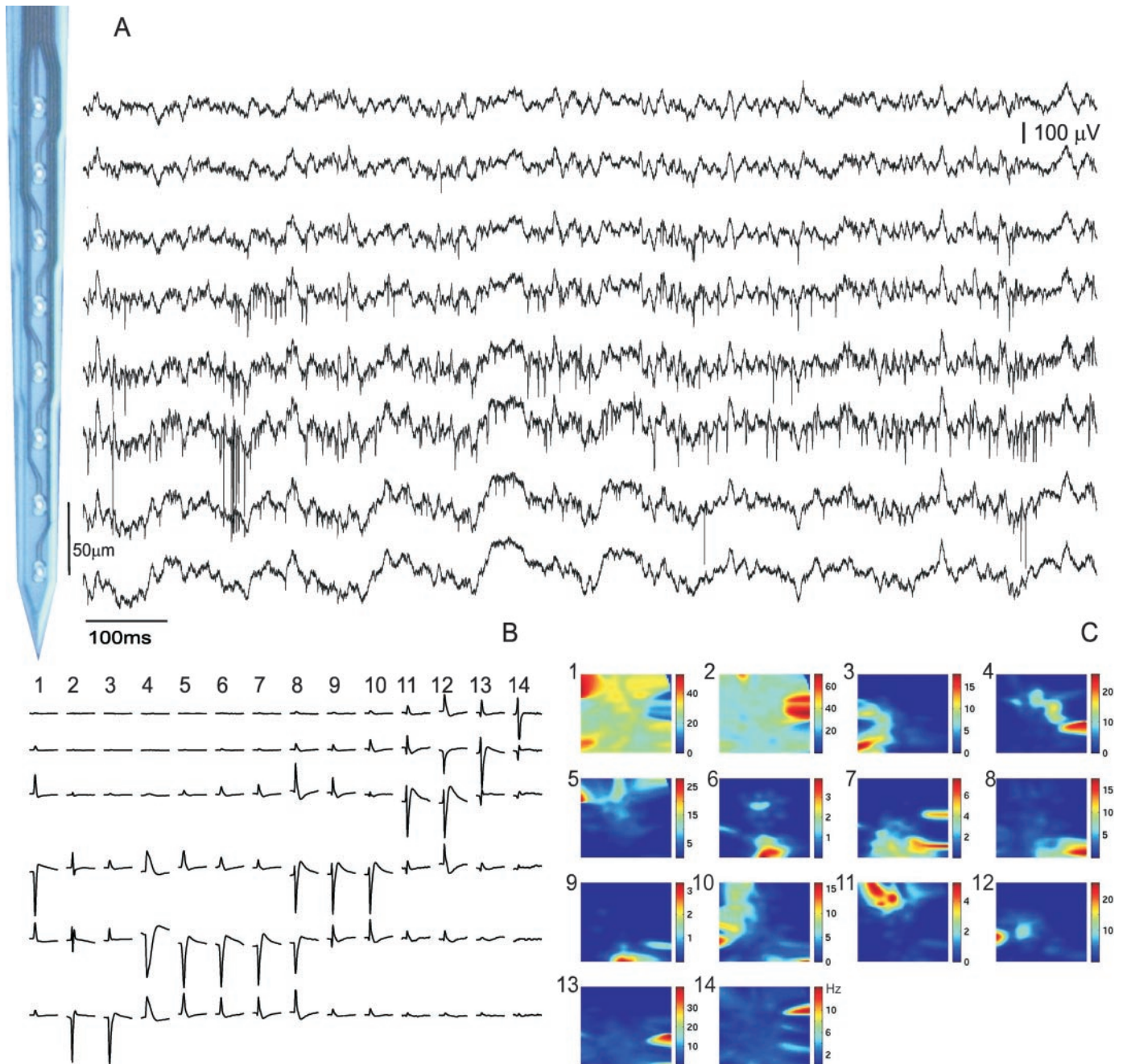


FIG. 5. Recording unit and field activity with a 64-site active probe in the behaving rat. *A*: recordings are shown from a single shank, spanning the CA1 pyramidal layer. *B*: CSD of units. Sinks are down. On the basis of spike shape, firing frequency and spike discharge dynamics units 1 and 2 were classified as putative interneurons and units 3–14 as pyramidal cells (Csicsvari et al. 1999). Note the different depth distribution of neurons. *C*: spatial “maps” of spike activity for each unit shown in *B* on an open field (40 × 50 cm). Firing rates are color-coded (Hz). Note similar size but different locations of place fields for pyramidal cells.

DISCUSSION

Parallel recording of neuronal activity in the intact brain is a prerequisite for our understanding of neuronal representation and storage of information. Micro-machined silicon microelectrode arrays are particularly promising for achieving this goal. The two-dimensional probes described here provided exceptionally high-density recording of unit and field activity with minimal tissue displacement or damage. The on-chip active circuit eliminated movement and other artifacts and greatly reduced the mass of the headgear. The precise geometry of the

recording tips allowed for the estimation of the spatial location of the recorded neurons.

Massively parallel recording of single units with silicon arrays

To date, methods for efficient spatial and temporal resolution of neuronal activity in the depth of the brain have been limited to recording from multiple single cells with closely spaced sensors. With these methods, the number of recording

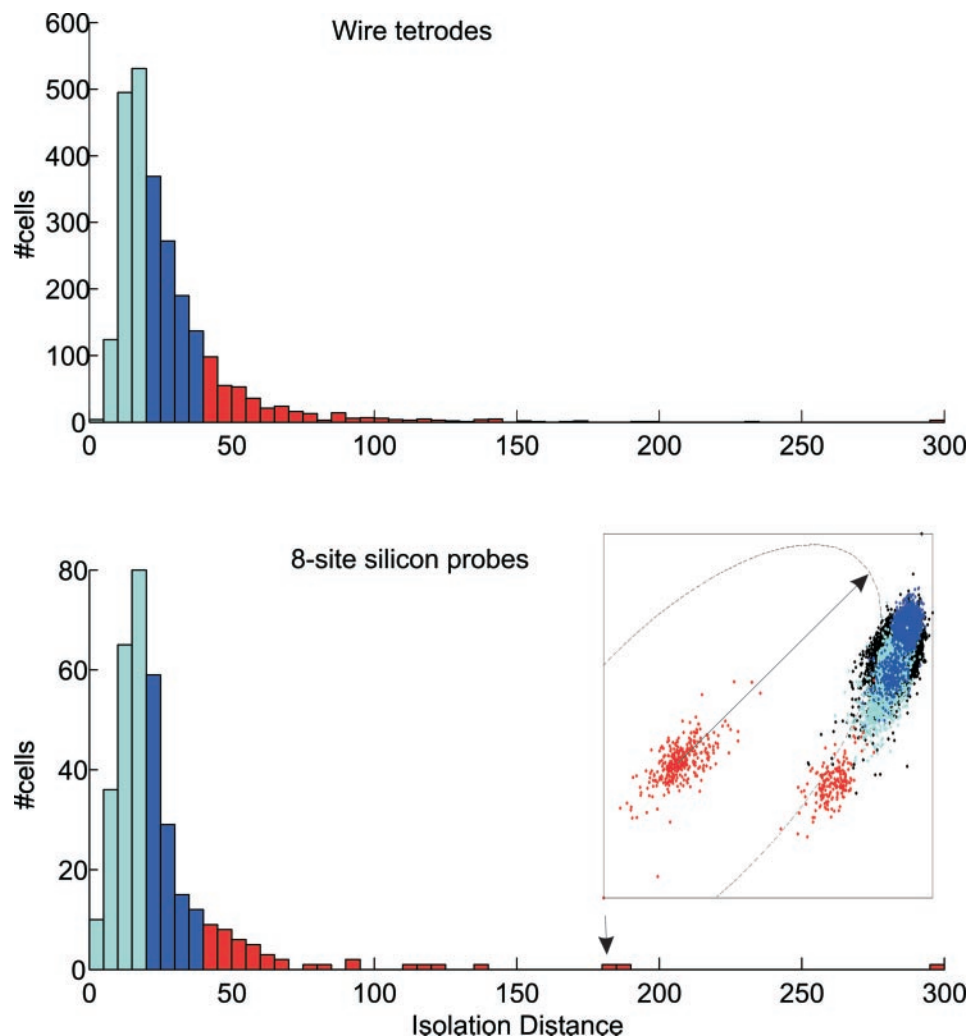


FIG. 6. Unit separation quality in the hippocampal CA1 region is similar with tetrode and silicon probe recordings. Quality of clusters ("isolation distance") was estimated by measuring the Mahalanobis distance from the cluster center within which as many points belong to other clusters as belong to the specified cluster (see *inset*). Clusters on the basis of isolation distance measure were designated as poor ("reject;" light blue), acceptable (dark blue), and excellent (red). To ensure that the comparison was not biased toward the multi-site probes, the same number of features ($n = 12$) was used to compute isolation distance in both cases. Clusters for tetrodes were obtained from Harris et al. (2000, 2002).

sites and the amount of tissue damage, isolation quality, and long-term stability compete with each other. Recording from large numbers of neurons distributed broadly over the cortex and other cortical region regions is possible with wire electrodes (Deadwyler and Hampson 1995; Hoffman and McNaughton 2002; Kralik et al. 2001; Nicolelis et al. 1997). However, recording from a physiologically representative portion of cells from a small piece of tissue to obtain insight into the operations of local networks requires a different approach. In addition to the large number of parallel-recorded units, it is important to acquire information about their spatial layout and, preferably, their cell type identity. The two-dimensional silicon probes described here fulfill some of these requirements. First, the tissue displacement and damage inflicted by a silicon probe is significantly less than that of a wire tetrode. The diameter of a twisted tetrode is 35–50 μm (i.e., $\sim 1,800 \mu\text{m}^2$ tip surface area), and the tips of tetrodes often splay apart after chronic implantation (Jog et al. 2002). The blunt area of the tetrode tip is twice as large as that of the silicon probe at its uppermost site (for 8-site shanks) and three to five times larger than the tip of the silicon probe. The tapered feature of the silicon shank further reduces damage on depth advancement of the probe. Because all shanks are moved simultaneously in the brain, the effects of differential drifts at various recording sites, inherent

in multiple tetrode recordings, are reduced, thus improving recording stability.

The recording sites of the probe can directly line up parallel with the somata and dendrites. Because the voltage is inversely proportional to distance from the soma, the voltage gradient across the recording sites provides an approximate location of the cell body of the recorded neuron (Henze et al. 2000; Holt and Koch 1999). The known geometry of the recording sites in multiple shank recordings provides precise information about the lateral distances of the recorded units, i.e., whether they are in the same or different micro-architectural areas, such as columns or barrels. In addition to spike occurrence, several intracellular features, such as the maximum rate of depolarization and repolarization of the action potential, relative polarization state of the membrane from rest, and the speed and extent of somadendritic back-propagation of the action potential can be estimated from the features of the extracellularly recorded spikes (Buzsáki et al. 1996; Henze et al. 2000). The co-linear arrangement of the recording sites allows for the estimation of high spatial resolution CSD. For unit separation, this is an added advantage because it eliminates electromyographic noise, which can be substantial in rats and mice due to the close proximity of the large masseter muscles to the recording sites, and other high-frequency electronic noise. Im-

portantly, high spatial resolution of local currents is important not only for investigation of network rules but can be exploited for practical purposes as well, e.g., controlling prosthetic devices (Pesaran et al. 2002).

Spikes of pyramidal shaped neurons generate an extracellular dipole parallel with the somadendritic axon of the neuron (Drake et al. 1988; Nádasdy et al. 1998). The extracellular spike can be monitored several hundred micrometers away in the vertical direction. In the horizontal direction, pyramidal cells can be detected $\leq 100 \mu\text{m}$ from the recording site (Henze et al. 2000; Jog et al. 2002). In support of these previous observations, we rarely recorded from the same putative pyramidal cell with neighboring shanks of the 64-site probe. Therefore 200- μm shank separation appears adequate for maximum sampling of the pyramidal cell population in the cortex of the rat. In the hippocampal CA1 region a 64-site probe can record, in principle, from all neurons in a $200 \times 1,400 \mu\text{m}$ strip of tissue, provided that all eight shanks are properly positioned in the pyramidal layer. A remaining fundamental problem is adequate separation of single cells (Harris et al. 2000) that can be improved by increasing spatial sampling further (see following text) and by developing novel spike-sorting algorithms. The high dimensionality of multiple-site monitoring of single-unit activity by silicon probes requires spike sorting methods that are fundamentally different from the currently used ones for tetrode architectures.

Increasing the number of recording sites inevitably increases the size and weight of the headstage carried by the small animal. For wire electrodes, independently movable drives are needed for each electrode for the exact positioning of the recording tips near the cell bodies. In addition, each high-impedance wire should be buffered to reduce low-frequency noise. With a large number of electrodes, this not only increases the weight but also the length of the interconnects, making the biological signal vulnerable to various artifacts. The high-density, two-dimensional probes used in this study require only a single microdrive for positioning. The vertical span of the eight recording sites is sufficient so that most or all shanks can be placed in the same layer even if the structure is curved, such as the hippocampal CA1 pyramidal layer. In the neocortex, all sites of all shanks recorded extracellular units. A further considerable reduction in volume and weight is due to the on-chip electronics that eliminates the need of preamplifiers. The low-impedance outputs of the active silicon probes can be directly connected to high-density connectors. Besides volume and weight reduction, the most important advantage of on-chip circuitry is the reduction of movement and environment-derived artifacts due to the substantially reduced interconnect lengths between the recording sites and preamplifier inputs. Although in the present experiments the amplifiers provided only unity gain, amplification by 10 or 100 is possible using essentially the same circuitry (Olsson et al. 2002).

The triangulation method of unit clustering is based on the tacit assumption that neurons are point sources of the extracellularly recorded currents. Therefore best separation is expected from three-dimensional monitoring devices (McNaughton et al. 1983; Recce and O'Keefe 1989). To obtain maximum unit separation, the recording sites should be evenly separated in all three dimensions. However, this requirement is not met by either the silicon probes tested here and or by wire tetrodes. Wire tetrode tips typically form a diamond shape on two-

dimensional surface (Jog et al. 2002). The site arrangements of the silicon probe form either a one- or two-dimensional array (staggered recording sites). The staggered sites have both vertical and horizontal (i.e., 2-dimensional) separation, mimicking wire tetrodes. Importantly, amplitude distribution of extracellular spikes is strongly biased by the morphology of neurons with vertically elongated fields for pyramidal cells (Henze et al. 2000). Therefore the efficacy of unit separation depends not only the recording site configuration but also the cytoarchitecture of the recorded neurons and whether the electrode approaches the cell body from the basal or apical dendrites. In the hippocampal CA3 region, similar cluster qualities were obtained by either wire tetrodes or one-dimensional (4-site) silicon probes (Csicsvari et al. 2000). Each neuron type may require different tip configurations for ideal unit isolation.

Outlook

An ideal recording electrode has a very small volume, so that tissue damage is minimized, but has very large number of monitoring sites so that the recorded spikes, emanating from different neurons, can be reliably separated. These competing demands limit the number of useful recording sites on a given shank. The microfabrication technology used here employed a 2- μm -wide interconnect lead (on 4- μm centers) per recording site (2 μm features). Thus >10 – 12 recording sites require a shank wide enough to produce noticeable tissue damage and less favorable conditions for unit recording. However, present industrial production uses 0.18- μm features and multiple levels of metal. Line widths as small as 22 nm are being targeted for the year 2010 (Geppert 2002). Clearly, interconnect will not limit the eventual realization of very large numbers of sites on probes displacing very small volumes of tissue. Indeed, the only reason for having any silicon under the present shanks (and not just the very thin dielectric layers encapsulating the interconnects) is the need for sufficient strength that allows the probes to penetrate brain tissue. Thus silicon probes are strength limited rather than technology limited in shrinking overall shank dimensions, and there is no doubt that probes will evolve to ever smaller feature sizes in coming years as they become more widely used in neurophysiological research. Recently, we have tested a 32-site, single-shank probe (50 μm vertical site separation), manufactured by double-sided deep reactive ion etching (DRIE) method with 1- μm interconnect lines and spacings (Norlin et al. 2002). Recordings from the neocortex and hippocampus yielded results similar to those presented in the preceding text. To utilize feature sizes consistent with present industrial practice, it is important to make the probes commercially available with fabrication in commercial foundries to help minimize the high tooling costs associated with manufacturing a limited number of probes for research.

Further development of on-chip interface circuitry is another important direction. Circuitry is needed to provide on-chip amplification, filtering, time-division multiplexing (Olsson et al. 2002), programmed microstimulation through the recording sites, and, potentially, in vivo, real-time signal processing. On-chip amplification can eliminate the need for expensive multichannel amplifier systems so that the probe output can be directly interfaced with a computer. These active interfaces will not only enhance the performance of silicon probes for basic research but are a prerequisite for fully implantable

neural prosthetic devices (Donoghue 2002; Nicolelis 2001; Rousche et al. 2001).

APPENDIX

Probe fabrication

The fabrication of probes with integrated CMOS circuitry was carried out with a merged bulk-micromachined 2P/1M CMOS process that has been described in detail elsewhere (Bai and Wise 2001; Gingerich et al. 2001). The probe body and shanks were defined with a deep boron diffusion which acted as an etch stop during the final release of probes from the wafer. A second boron diffusion of shorter duration allowed the definition of sharp probe tips, resulting in a rounded edge profile for the shanks. A stack of low-pressure chemical-vapor-deposited (LPCVD) silicon oxide/nitride/oxide insulated the polysilicon shank interconnects from the silicon substrate below and the tissue above. Through proper balancing of the compressive and tensile stresses of the oxide and nitride films, respectively, the residual stress in the shanks could be cancelled (Cho et al. 1992). This allowed the shanks to remain straight even when they are quite long (5 mm in the current probes). Normal CMOS circuit processing then followed. The bottom nitride layer in the dielectric stack acted as the masking nitride for field oxidation in the circuit area. A second polysilicon layer allowed the formation of poly/poly capacitors, which were used in the frequency compensation of the probe buffers. The circuit metal was a stacked Ti/Al layer, and TiN contact plugs were used to prevent junction spiking during circuit passivation with $\sim 1 \mu\text{m}$ of low-temperature oxide (LTO). A layer of sputtered or electroplated gold was then deposited on top of the LTO. This layer is helpful in reducing the optical sensitivity of the probe circuitry and was also used as a ground shield against (chemical and electrical) interference. Following patterning of the gold circuit shield, iridium recording sites were patterned by lift-off, and gold bonding pads were formed. Finally, a photoresist mask was applied to the completed probes, and the dielectrics between the probes were etched with reactive ion etching. The wafer was then thinned from the backside with an isotropic silicon etchant (a hydrofluoric acid and nitric acid mixture) and then immersed in a water/ethylene diamine pyrocatechol (EDP) mixture at 80°C . All areas of the wafer, not defined by the deep or shallow boron diffusions, were etched away, releasing the probes from the wafer. Circuit areas were protected from being attacked by the EDP with large guard rings of deep boron diffusion. Additional protection was provided at the corners of the circuit area using corner compensation (Puers and Sansen 1990) and dielectric bridges. When released, the probes were removed from EDP, rinsed thoroughly in de-ionized water, acetone, and isopropyl alcohol and then soaked overnight in methanol. The probes were then wire-bonded to a custom-designed printed circuit board and the bonds were potted in medical grade silicone to prevent body fluids from short-circuiting the contacts. Soldering pads along the edges of the printed circuit board served to connect the board to high-density (0.6 mm) connectors (Omnetics, Minneapolis, MN).

Noise reduction by on-chip buffering

The two major sources of noise in extracellular recording are externally coupled noise and the thermal (Johnson) noise intrinsic to the electrode itself. Successful extracellular neural recording requires buffering the neural signal at a location close to the recording site to minimize the effect of externally coupled noise. With passive probes and wire electrodes, the "antenna" effect of the interconnect (e.g., wire bonds, printed circuit board traces, connectors and in some cases cabling) between the recording site and buffer input is considerable, providing a means for capacitive and/or inductive noise coupling. On-chip buffering shortens the length of the high-impedance input node and decrease the magnitude of charge coupled into the input. A

headstage buffer is itself a source of noise, and it is desirable that this electronic noise be insignificant compared with the thermal electrode noise in the bandwidth of interest. The on-chip buffers in the current design exhibit a baseline noise of $6.4 \mu\text{V}$ in the 10-kHz bandwidth of interest. While some commercially available operation amplifiers have better noise characteristics, it is important to note that the intrinsic electrode noise ($12.7 \mu\text{V}$ for the iridium sites used in the present experiments) is significantly higher than the electronic noise of the preamplifier. Because independent noise sources add as the sum of squares, electronic noise contributes only 13% to the total baseline noise level.

We thank P. Norlin for the gift of 32-site linear probes.

Present addresses: J. Csicsvari, MRC Anatomical Neuropharmacology Unit, Dept. of Pharmacology, Oxford University, Mansfield Road, Oxford OX1 3TH, UK; D. A. Henze, Merck Research Laboratories, West Point, PA, 19486; B. Jamieson, Detector Systems Branch, NASA/ Goddard Space Flight Center, Greenbelt, MD 20771.

DISCLOSURES

This work was supported by National Institutes of Health Grants NS-34994, NS-43157, MH-54671, NO1-NS-0-2329, and 1P41RR-09754.

REFERENCES

- Andersen P, Bliss TV, Lomo T, Olsen LI, and Skrede KK. Lamellar organization of hippocampal excitatory pathways. *Acta Physiol Scand*. 76: 4A–5A, 1969.
- Bai Q and Wise KD. Single-unit neural recording with active microelectrode arrays. *IEEE Trans Biomed Eng* 48: 911–920, 2001.
- Bragin A, Jandó G, Nádasdy Z, Hetke J, Wise K, and Buzsáki G. Gamma (40–100 Hz) oscillation in the hippocampus of the behaving rat. *J Neurosci* 15: 47–60, 1995.
- Buzsáki G, Grastyán E, Czopf J, Kellényi L, and Prohaska O. Changes in neuronal transmission in the rat hippocampus during behavior. *Brain Res* 225: 235–247, 1981.
- Buzsáki G, Horvath Z, Urioste R, Hetke J, and Wise K. High-frequency network oscillation in the hippocampus. *Science* 256: 1025–1027, 1992.
- Buzsáki G and Kandel A. Somadendritic backpropagation of action potentials in cortical pyramidal cells of the awake rat. *J Neurophysiol* 79: 1587–1591, 1998.
- Buzsáki G, Penttonen M, Nádasdy Z, and Bragin A. Pattern and inhibition-dependent invasion of pyramidal cell dendrites by fast spikes in the hippocampus in vivo. *Proc Natl Acad Sci USA* 93: 9921–9925, 1996.
- Castro-Alamancos MA and Connors BW. Cellular mechanisms of the augmenting response: short-term plasticity in a thalamocortical pathway. *J Neurosci* 16: 7742–7756, 1996.
- Chicurel M. Windows on the brain. *Nature* 412: 266–268, 2001.
- Cho ST, Najafi K, and Wise K. Internal stress compensation and scaling in ultrasensitive silicon pressure sensors. *IEEE Trans Electron Devices* 39: 836–842, 1992.
- Churchland PS and Sejnowski TJ. *The Computational Brain*. Cambridge, MA: MIT Press, 1992.
- Csicsvari J, Hirase H, Czurkó A, and Buzsáki G. Reliability and state dependence of pyramidal cell-interneuron synapses in the hippocampus: an ensemble approach in the behaving rat. *Neuron* 21: 179–189, 1998.
- Csicsvari J, Hirase H, Czurkó A, Mamiya A, and Buzsáki G. Oscillatory coupling of hippocampal pyramidal cells and interneurons in the behaving rat. *J Neurosci* 19: 274–287, 1999.
- Csicsvari J, Hirase H, Mamiya A, and Buzsáki G. Ensemble patterns of hippocampal CA3–CA1 neurons during sharp wave-associated population events. *Neuron* 28: 585–594, 2000.
- Csicsvari J, Jamieson B, Wise K, and Buzsáki G. Mechanisms of gamma oscillations in the hippocampus in vivo. *Neuron* 2003.
- Deadwyler SA and Hampson RE. Ensemble activity and behavior: what's the code? *Science* 270: 1316–1318, 1995.
- Do VM, Martinez CO, Martinez JL Jr, and Derrick BE. Long-term potentiation in direct perforant path projections to hippocampal CA3 regions in vivo. *J Neurophysiol* 87: 669–678, 2002.
- Donoghue JP. Connecting cortex to machines: recent advances in brain interfaces. *Nat Neurosci* 5, Suppl: 1085–1088, 2002.

- Drake KL, Wise KD, Farraye J, Anderson DJ, and BeMent SL.** Performance of planar multisite microprobes in recording extracellular single-unit intracortical activity. *IEEE Trans Biomed Eng* 35: 719–732, 1988.
- Eichenbaum H and Davis JL.** *Neuronal Ensembles: Strategies for Recording and Decoding*. New York: Wiley-Liss, 1988.
- Evarts EV.** A technique for recording activity of subcortical neurons in moving animals. *Electroencephalogr Clin Neurophysiol* 24: 83–86, 1968.
- Geppert L.** The amazing vanishing transistor act. *IEEE Spectrum* 39: 28–33, 2002.
- Gingerich MD, Hetke JF, Anderson DJ, and Wise KD.** A 256-Site 3D CMOS microelectrode array for multipoint stimulation and recording in the central nervous system. *International Conference on Solid-State Sensors and Actuators (Transducers'01)*, Munich, Germany, 2001.
- Gray CM, Maldonado PE, Wilson M, and McNaughton B.** Tetraodes markedly improve the reliability and yield of multiple single-unit isolation from multi-unit recordings in rat striate cortex. *J Neurosci Methods* 63: 43–54, 1995.
- Hampson RE, Simeral JD, and Deadwyler SA.** Distribution of spatial and nonspatial information in dorsal hippocampus. *Nature* 402: 610–614, 1999.
- Hampson RE, Simeral JD, and Deadwyler SA.** What ensemble recordings reveal about functional hippocampal cell encoding. *Prog Brain Res* 130: 345–357, 2001.
- Harris KD, Henze DA, Csicsvari J, Hirase H, and Buzsáki G.** Accuracy of tetraode spike separation as determined by simultaneous intracellular and extracellular measurements. *J Neurophysiol* 84: 401–414, 2000.
- Harris KD, Hirase H, Leinekugel X, Henze DA, and Buzsáki G.** Temporal interaction between single spikes and complex spike bursts in hippocampal pyramidal cells. *Neuron* 32: 141–149, 2001.
- Harris KD, Henze DA, Hirase H, Leinekugel X, Dragoi G, Czurko A, and Buzsáki G.** Spike train dynamics predicts theta-related phase precession in hippocampal pyramidal cells. *Nature* 417: 738–741, 2002.
- Henze DA, Borhegyi Z, Csicsvari J, Mamiya A, Harris KD, and Buzsáki G.** Intracellular features predicted by extracellular recordings in the hippocampus in vivo. *J Neurophysiol* 390–400, 2000.
- Hirase H, Leinekugel X, Csicsvari J, Czurko A, and Buzsáki G.** Behavior-dependent states of the hippocampal network affect functional clustering of neurons. *J Neurosci* 21: RC145, 2001.
- Hoffman KL and McNaughton BL.** Coordinated reactivation of distributed memory traces in primate neocortex. *Science* 297: 2070–2073, 2002.
- Holsheimer J.** Electrical conductivity of the hippocampal CA1 layers and application to current-source-density analysis. *Exp Brain Res* 67: 402–410, 1987.
- Holt GR and Koch C.** Electrical interactions via the extracellular potential near cell bodies. *J Comput Neurosci* 6: 169–184, 1999.
- Jog MS, Connolly CI, Kubota Y, Iyengar DR, Garrido L, Harlan R, and Graybiel AM.** Tetraode technology: advances in implantable hardware, neuroimaging, and data analysis techniques. *J Neurosci Methods* 117: 141–152, 2002.
- Kandel A and Buzsáki G.** Cellular-synaptic generation of sleep spindles, spike-and-wave discharges, and evoked thalamocortical responses in the neocortex of the rat. *J Neurosci* 17: 6783–6797, 1997.
- Kralik JD, Dimitrov DF, Krupa DJ, Katz DB, Cohen D, and Nicolelis MA.** Techniques for long-term multisite neuronal ensemble recordings in behaving animals. *Methods* 25: 121–150, 2001.
- Kristensen BW, Noraberg J, Thiebaud P, Koudelka-Hep M, and Zimmer J.** Biocompatibility of silicon-based arrays of electrodes coupled to organotypic hippocampal brain slice cultures. *Brain Res* 896: 1–17, 2001.
- Kuperstein M and Eichenbaum H.** Unit activity, evoked potentials and slow waves in the rat hippocampus and olfactory bulb recorded with a 24-channel microelectrode. *Neuroscience* 15: 703–712, 1985.
- Lang EJ, Sugihara I, Welsh JP, and Linas R.** Patterns of spontaneous purkinje cell complex spike activity in the awake rat. *J Neurosci* 19: 2728–2739, 1999.
- Mao BQ, Hamzei-Sichani F, Aronov D, Froemke RC, and Yuste R.** Dynamics of spontaneous activity in neocortical slices. *Neuron* 32: 883–898, 2001.
- McNaughton BL, O'Keefe J, and Barnes CA.** The stereotrode: a new technique for simultaneous isolation of several single units in the central nervous system from multiple unit records. *J Neurosci Methods* 8: 391–397, 1983.
- Mountcastle VB.** The columnar organization of the neocortex. *Brain* 120: 701–722, 1997.
- Nádasdy Z, Csicsvari J, Penttonen M, Hetke J, Wise K, and Buzsáki G.** Extracellular recording and analysis of neuronal activity: from single cells to ensembles. In: *Large Scale Recording of Neuronal Activity*, edited by Eichenbaum H and Davis JL. New York: Wiley, 1998, p. 17–55.
- Najafi K, Ji J, and Wise KD.** Scaling limitations of silicon multichannel recording probes. *IEEE Trans Biomed Eng* 37: 1–11, 1990.
- Najafi K and Wise KD.** An implantable multielectrode array with on-chip signal processing. *IEEE J Solid-State Circuits* 21: 1035–1045, 1986.
- Nicholson C and Freeman JA.** Theory of current source-density analysis and determination of conductivity tensor for anuran cerebellum. *J Neurophysiol* 38: 356–368, 1975.
- Nicolelis MA, Ghazanfar AA, Faggin BM, Votaw S, and Oliveira LM.** Reconstructing the engram: simultaneous, multisite, many single neuron recordings. *Neuron* 18: 529–537, 1997.
- Nicolelis MA.** Actions from thoughts. *Nature* 409, Suppl: 403–407, 2001.
- Norlin P, Kindlundh M, Mouroux A, Yoshida K, and Hofmann UG.** A 32-site neuronal probe fabricated by DRIE of SOI substrates. *J Micromech Microeng* 12: 414–419, 2002.
- Olsson RH III, Gulari MN, and Wise KD.** Silicon neural recording arrays with on-chip signal processing for in-vivo data acquisition. *Proceedings of the 2nd Annual IEEE-EMBS Conference on Microtechnology Medicine and Biology*, Capri, Italy, p. 237–240, 2002.
- Pesaran B, Pezaris JS, Sahani M, Mitra PP, and Andersen RA.** Temporal structure in neuronal activity during working memory in macaque parietal cortex. *Nat Neurosci* 5: 805–811, 2002.
- Petsche H, Pockberger H, and Rappelsberger P.** On the search for the sources of the electroencephalogram. *Neuroscience* 11: 1–27, 1984.
- Puers B and Sansen W.** Compensation structures for convex corner micro-machining in silicon. *Sensors Actuators A* 23: 1036–1041, 1990.
- Quirk MC, Blum KI, and Wilson MA.** Experience-dependent changes in extracellular spike amplitude may reflect regulation of dendritic action potential back-propagation in rat hippocampal pyramidal cells. *J Neurosci* 21: 240–248, 2001.
- Recce M and O'Keefe J.** The tetraode: a new technique for multiunit extracellular recording. *Soc Neurosci Abstr* 15: 1270, 1989.
- Redish AD, Battaglia FP, Chawla MK, Ekstrom AD, Gerrard JL, Lipa P, Rosenzweig ES, Worley PF, Guzowski JF, McNaughton BL, and Barnes CA.** Independence of firing correlates of anatomically proximate hippocampal pyramidal cells. *J Neurosci* 21: RC134, 2001.
- Rice FL and Van der Loos H.** Development of the barrels and barrel field in the somatosensory cortex of the mouse. *J Comp Neurol* 171: 545–560, 1977.
- Rusche PJ, Pellinen DS, Pivin DP Jr, Williams JC, Vetter RJ, and Kipke DR.** Flexible polyimide-based intracortical electrode arrays with bioactive capability. *IEEE Trans Biomed Eng* 48: 361–371, 2001.
- Steriade M.** Corticothalamic resonance, states of vigilance and mentation. *Neuroscience* 101: 243–276, 2000.
- Szabó I, Czurko A, Csicsvari J, Hirase H, Leinekugel X, and Buzsáki G.** The application of printed circuit board technology for fabrication of multi-channel micro-drives. *J Neurosci Methods* 105: 105–110, 2001.
- Szentágothai J.** The “module-concept” in cerebral cortex architecture. *Brain Res* 95: 475–496, 1975.
- Wilson MA and McNaughton BL.** Dynamics of the hippocampal ensemble code for space. *Science* 261: 1055–1058, 1993.
- Wilson MA and McNaughton BL.** Reactivation of hippocampal ensemble memories during sleep. *Science* 265: 676–679, 1994.
- Wise KD and Najafi K.** Microfabrication techniques for integrated sensors and microsystems. *Science* 254: 1335–1342, 1991.
- Ylinen A, Bragin A, Nádasdy Z, Jandó G, Szabó I, Sík A, and Buzsáki G.** Sharp wave-associated high-frequency oscillation (200 Hz) in the intact hippocampus: network and intracellular mechanisms. *J Neurosci* 15: 30–46, 1995.